Production of very cold neutrons

V. V. Golikov, V. I. Lushchikov, and F. L. Shapiro
Joint Institute for Nuclear Research
(Submitted July 12, 1972)
Zh. Eksp. Teor. Fiz. **64**, 73-81 (January 1973)

The output of very cold neutrons (VCN) from different thin plates-converters at temperature T_c exposed to an isotropic thermal-neutron flux with a Maxwellian spectrum at temperature T_n is calculated. It is shown that for a number of media (polyethylene, zirconium hydride, beryllium, etc.) the VCN output at fixed T_n increases appreciably as the converter is cooled. The VCN yield of aluminum and magnesium is not very dependent on T_c and this is connected with the relatively low neutron heating cross section as compared with the capture cross section of these media. It is concluded that, when the VCN are obtained from a thin surface layer of the moderator, it is sufficient to cool the surface layer or the converter and not the moderator as a whole. The calculations have been verified experimentally using the VCN channel of the pulsed IBR-30 reactor. The measured VCN yields of different converters are found to be in agreement with the calculations. The cooling of polyethylene or zirconium hydride converters from room temperature down to 130°K and 90°K was found to lead to a smaller increase in the VCN flux than was predicted by the calculations.

In our previous papers[1,2] very cold neutrons (VCN), i.e., neutrons with energies $E \sim 10^{-7}$ eV, were obtained from a thin-plate converter exposed to the thermal neutron flux. It is well known that an increased VCN output can be obtained from a reactor by cooling the moderator. In the case of VCN obtained from a thin surface layer of the moderator, which is of the order of the VCN mean free path (< 5 mm), it is sufficient to cool only this surface layer, or the converter, and not the moderator as a whole.[3,4]

We have calculated the VCN output of different converters at temperature T_c exposed to an isotropic thermal-neutron flux with a Maxwellian spectrum at temperature T_n. A partial experimental verification of the calculations was carried out in the VCN channel of the pulsed IBR-30 reactor.

1. METHOD OF CALCULATION

Consider a flat converter inside the horizontal VCN channel (Fig. 1). As a result of total reflection, all neutrons leaving the converter with energy

$$E < U_w \equiv (4\hbar^2/m)\pi n_w b_w$$

can propagate along the channel, where n_w is the density of nuclei, b_n is the coherent neutron scattering length of the channel wall, m is the neutron mass, and for copper walls $U_n \approx 1.7 \times 10^{-7}$ eV. The flux of neutrons with energies between E and E + dE leaving 1 cm^2 of a converter of thickness d can be written in the form

$$\Phi(E)dE = dE\int_0^\infty \Phi_T(E')n_c\sigma(E'\to E)dE'\int_0^d dx\int_0^{\pi/2} W(E,x,\theta)\frac{2\pi\sin\theta\,d\theta}{4\pi}. \quad (1)$$

In this expression $\Phi_T(E')dE'$ is the flux of neutrons with energies between E' and E' + dE' which are intercepted by the converter (we are assuming that this flux is uniform throughout the volume of the converter), n_c is the density of nuclei in the converter, $\sigma(E' \to E)dE$ is the cross section for the inelastic scattering of neutrons with energy E' into the energy interval E + dE,

$$W(E,x,\theta) = \exp\left(-\frac{xn_c\sigma_t(E)}{\cos\theta}\right)$$

is the probability of escape of a neutron of energy E from a layer dx at a distance x from the surface of the converter, θ is the angle between the normal to the converter surface and the direction of escape of the neutron, and $\sigma_t(E)$ is the total neutron cross section of the converter material. For the moment, we are ignoring the reflection of neutrons from the converter-vacuum boundary.

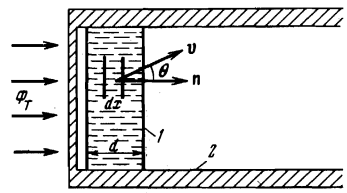

FIG. 1. Initial part of the neutron guide for very cold neutrons: 1—VCN converter exposed to the isotropic neutron flux, 2—vacuum neutron guide.

Integrating Eq. (1) with respect to x and θ and assuming that the converter thickness is $d \gg 1/n_c\sigma_t$, we obtain the total VCN flux in the energy range between zero and U_w:

$$\Phi = \frac{1}{4}\int_0^{U_w}\frac{dE}{\sigma_t(E)}\int_0^\infty \Phi_T(E')\cdot\sigma(E'\to E)dE'. \quad (2)$$

Direct utilization of Eq. (2) for calculating the VCN output of different converters is not possible because of the absence of experimental data on the cross sections σ_t and $\sigma(E' \to E)dE$ in a broad range of energies and converter temperatures. We note, however, that by virtue of the 1/v law, the capture cross section σ_c and the inelastic VCN cross section

$$\sigma_{ne} = \int_0^\infty \sigma(E\to E')dE'$$

are much higher than the elastic cross section. Therefore, using the principle of detailed balancing

$$\sigma(E\to E')E\exp(-E/T_c) = \sigma(E'\to E)E'\exp(-E'/T_c),$$

we can write the total cross section in the form

$$\sigma_t(E) \approx \sigma_c + \sigma_{ne} \quad (3)$$
$$= [\sigma_c(E_0)E_0^{1/2}]E^{-1/2} + E^{-1/2}\int_0^\infty [\sigma(E'\to E)E^{-1/2}]E'\exp\left(-\frac{E'-E}{T_c}\right)dE'.$$

All the quantities in the square brackets in Eq. (3) are independent of E, and E_0 is a certain fixed energy.

Substituting Eq. (3) in Eq. (2), and assuming that the converter is exposed to a Maxwellian spectrum of thermal neutrons having a total flux Φ_0 and temperature T_n, i.e.,

$$\Phi_T(E') = \frac{\Phi_0}{T_n^2} E' \exp\left(-\frac{E'}{T_n}\right),$$

we find that when $E \ll T_c$

$$\Phi = \frac{1}{4}\Phi_0 \int_0^{U_w} EG(T_n, T_c)\,dE = \frac{1}{8}\Phi_0 U_w^2 G(T_n, T_c), \tag{4}$$

where

$$G(T_n, T_c) = T_n^{-2} \int_0^\infty E'[\sigma(E' \to E)E^{-1/2}]\exp\left(-\frac{E'}{T_n}\right)dE'$$

$$\times\left\{[\sigma_c(E_0)E_0^{1/2}] + \int_0^\infty [\sigma(E' \to E)E^{-1/2}]E' \exp(-E'/T_c)\,dE'\right\}^{-1} \tag{5}$$

is independent of the energy E of the escaping VCN, and is determined only by the converter characteristics.

The inelastic cross section in $G(T_n, T_c)$ can be calculated by using the single-phonon incoherent approximation.[5] In this way we obtain

$$G(T_n, T_c) = \frac{1}{T_n^2}\int_0^\infty E'^{1/2} g(E')\exp\left(-\frac{E'}{T_n}\right)\left(1-\exp\left(-\frac{E'}{T_c}\right)\right)^{-1} dE' \cdot$$

$$\times\left\{\sigma_c(E_0)E_0^{1/2}\,\sigma_s^{-1}A + \int_0^\infty E'^{1/2} g(E')\exp\left(-\frac{E'}{T_c}\right)\left(1-\exp\left(-\frac{E'}{T_c}\right)\right)^{-1} dE'\right\}^{-1}, \tag{6}$$

where g(E') is the normal vibration spectrum of the converter, σ_s is the total scattering cross section of the bound converter nuclei, and A is the converter mass number. In deriving Eq. (6), we assumed that the Debye-Waller factor was unity.

In the absence of capture, and when the neutron gas temperature is equal to the converter temperature, we find from Eq. (4) that

$$\Phi = \frac{\Phi_0}{8}\frac{U_w^2}{T_n^2},$$

which corresponds to the area of the VCN region in the thermal-neutron spectrum.

Calculations of $G(T_n, T_c)$ for a number of converter materials are shown in Tables I–V and in Fig. 2 [for convenience, the function $G(T_n, T_c)$ is normalized so that it is equal to unity for polyethylene at $T_c = T_n = 300°K$]. The frequency spectra were taken from[6-9]. The accuracy of the calculations can be judged, to some extent, from Fig. 3, which shows the calculated and experimental[5,10] inelastic scattering cross sections $\sigma_{ne}E^{1/2}$ connected with the neutron heating.

Calculations have shown that when multiphonon scattering is taken into account. this does not affect $G(T_n, T_c)$ by more than 15%. The use of the incoherent approximation for such coherent scatterers as Al, Mg, and Be might give rise to some reservations. However, it was noted, for example, in[5] that the correction for interference effects in the case of an integral parameter such as the total inelastic cross section does not exceed 20% in the majority of media.

It is clear from Fig. 2 that, in the case of polyethylene, zirconium hydride, and beryllium, the VCN output at constant neutron-spectrum temperature increases appreciably as the converter is cooled down. This phenomenon is explained by the fact that, as T_c decreases, the VCN heating cross section [second term in the denominator of Eq. (6)] decreases more rapidly than the thermal-neutron cooling cross section [numerator in Eq. (6)]. The VCN output of Al and Mg, on the other hand, is not very dependent on the converter temperature. This is connected with the relatively low neutron heating cross section as compared with the capture cross section of these media.

At fixed converter temperature, the VCN yield is not very dependent on the neutron temperature: as T_n decreases, the neutron cooling cross section is also found to decrease (owing to the contraction of the part of the frequency spectrum employed), and this largely compen-

TABLE I. $G(T_n, T_c)$ for polyethylene

T_n, °K	T_c, °K						
	4	20	40	80	150	220	300
20	6.7	7.2	7.8	5.6	2.8	2.2	1.7
40	13.9	13.9	12.8	7.8	3.9	2.8	2.0
70	20.0	19.4	16.7	9.4	4.4	2.8	2.0
100	22.2	21.7	17.8	9.4	3.9	2.8	1.6
150	21.6	21.1	17.2	8.9	3.3	2.2	1.5
200	20.5	20.0	16.1	7.8	3.3	1.6	1.1
250	18.9	18.3	15.0	7.2	2.8	1.6	1.1
300	17.8	17.2	13.9	6.6	2.8	1.6	1

TABLE II. $G(T_n, T_c)$ for beryllium

T_n, °K	T_c, °K						
	4	20	40	80	150	220	300
20	0.3	0.3	0.4	0.5	0.28	0.17	0.11
40	0.8	0.8	0.9	0.9	0.4	0.2	0.17
70	2.2	2.2	2.2	2.1	0.9	0.4	0.2
100	5.0	5.0	5.0	4.2	1.6	0.7	0.4
150	10.0	10.0	9.4	8.3	3.0	1.3	0.7
200	13.3	13.3	13.3	11.1	3.9	1.7	+0.9
250	15	15	14.4	12	4.4	1.8	1
300	15	15	15	12.5	4.4	1.8	1

TABLE III. $G(T_n, T_c)$ for aluminum

T_n, °K	T_c, °K								
	4	20	40	80	150	220	300	400	500
20	0.02	0.02	0.02	0.03	0.05	0.07	0.08	0.10	0.12
40	0.05	0.05	0.06	0.07	0.09	0.11	0.14	0.16	0.18
70	0.11	0.11	0.11	0.12	0.15	0.18	0.22	0.25	0.28
100	0.14	0.14	0.14	0.15	0.18	0.21	0.25	0.29	0.32
150	0.14	0.14	0.14	0.15	0.18	0.20	0.23	—	—
200	0.12	0.12	0.13	0.13	0.15	0.17	0.20	0.24	0.27
250	0.11	0.11	0.11	0.11	0.13	0.14	0.16	—	—
300	0.09	0.09	0.09	0.09	0.11	0.12	0.14	0.17	0.18

TABLE IV. $G(T_n, T_c)$ for magnesium

T_n, °K	T_n, °K						
	4	20	40	80	150	220	300
20	0.45	0.45	0.55	0.7	0.8	0.8	0.8
40	1.4	1.4	1.5	1.6	1.6	1.55	1.5
70	2.3	2.3	2.3	2.3	2.2	2.1	2.0
100	2.4	2.4	2.4	2.3	2.2	2.0	1.9
150	2.0	2.0	2.0	1.9	1.7	1.6	1.5
200	1.55	1.55	1.55	1.5	1.3	1.2	1.2
250	1.2	1.2	1.2	1.2	1.0	0.9	0.9
300	1.0	1.0	1.0	0.9	0.80	0.7	0.7

TABLE V. $G(T_n, T_c)$ for zirconium hydride

T_n, °K	T_n, °K						
	4	20	40	80	150	220	300
20	0.9	1.0	1.3	1.8	2.2	1.7	1.0
40	1.4	1.4	1.7	2.0	2.2	1.7	1.0
70	1.8	1.8	1.9	2.1	2.1	1.6	0.9
100	1.8	1.8	1.9	1.9	1.9	1.4	0.8
150	1.8	1.8	1.8	1.8	1.6	1.2	0.6
200	2.3	2.3	2.3	2.2	1.8	1.2	0.6
250	3.2	3.3	3.3	3.0	2.3	1.4	0.7
300	4.3	4.5	4.5	4.1	3.0	1.8	0.9

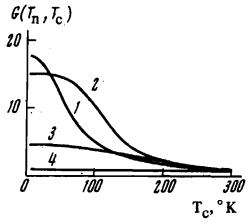

FIG. 2

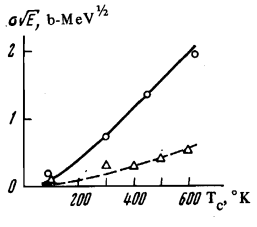

FIG. 3

FIG. 2. The dependence of $G(T_n, T_C)$ on the converter temperature. Neutron spectrum temperature $T_n = 300°K$. Curve 1—polyethylene, 2—beryllium, 3—zirconium hydride, 4—magnesium.

FIG. 3. Experimental and theoretical values of the heating cross section $\sigma_{ne}E^{1/2}$ for slow neutrons ($E < 1$ meV). Magnesium: O—experiment, solid curve—calculation; aluminum: Δ—experiment, broken curve—calculation.

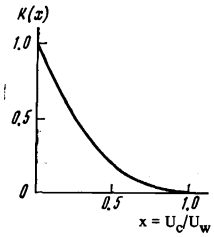

FIG. 4. VCN yield as a function of the ratio of the converter and neutron-guide wall potentials (U_C/U_W).

sates the factor T_n^{-2} in Eq. (6). It is also important to note that, in contrast to the cooling of a converter, the cooling of the moderator at constant reactor power leads to a reduction in the thermal flux Φ_0 because of constructional factors, and because the neutron density remains constant during cooling of moderators with diffusion length which is small in comparison with the slowing-down length and the size of the moderator, whereas the flux decreases as $T_n^{1/2}$. Therefore, only the converter need be cooled in VCN sources.

To compare the relative VCN yield of different converters, it is important to take into account the VCN reflection from the converter-vacuum separation boundary. Since the change in the neutron energy across the converted-vacuum boundary is $U_C - (4\hbar^2/m)\pi n_c b_c$, we have, instead of Eq. (4)

$$\Phi = \frac{\Phi_0}{4} G(T_n, T_C) \int_0^{U_W - U_C} E T_{12}(E)\, dE, \tag{7}$$

where

$$T_{12}(E) = {}^3/_2 y^{1/2}((y+1)^{1/2} - y^{1/2} - {}^1/_2 y^{1/2}), \quad y = E/U_C. \tag{8}$$

is the VCN transmission factor averaged over the angles at the converter-vacuum boundary (E is the neutron energy inside the converter), and the converter potential U_C is positive. Integration of Eq. (7) yields

$$\Phi = \frac{\Phi_0}{8} U_W^2 K\left(\frac{U_C}{U_W}\right) G(T_n, T_C),$$

$$K(x) = \frac{(1-x^{1/2})}{12x^2}(3x^3 + 2x^2 - 24x + 16) + \frac{x^2}{8}\ln\frac{1+(1-x)^{1/2}}{1-(1-x)^{1/2}} - \frac{4}{3}\frac{(1-x^2)(1-x)^2}{x^2}. \tag{9}$$

Equation (9) gives the total directed VCN flux leaving the converter into the neutron guide. The VCN flux recorded by the detector corresponds to Eq. (9) only in the case of a perfectly reflecting nonabsorbing neutron guide. According to[1,2], the propagation of VCN along a real neutron guide can be described in terms of the elementary diffusion theory. The neutron guide is characterized by two parameters, namely, the diffusion coefficient D and the diffusion length L.

We shall assume that the directed flux is converted into a diffuse flux near the converter. We can then use the balance of fluxes on the converter-vacuum boundary, and the boundary conditions for the diffusion equation, and hence deduce the diffuse VCN flux at the detector:

$$\Phi = \frac{\Phi_0}{4} G(T_n, T_C) \int_0^{U_W - U_C} \frac{E T_{12} e^{-l/L}\, dE}{T_{21} + \alpha(1 - {}^1/_2 T_{21}')}, \tag{10}$$

where T_{21} and T_{21}' are the neutron transmission factors averaged over the angles at the vacuum-converter boundary for the isotropic and directed components of the diffusion flux, respectively:

$$T_{21} = T_{12} y / (1+y),$$

$$T_{21}' = y(4+5y) - \frac{2}{\pi}(5y-1)(1+y)\operatorname{arctg} y^{1/2} - \frac{10}{\pi} y^{1/2}\left(y + \frac{7}{15} - \frac{4}{15(1+y)}\right).$$

Next, $\alpha = 4D/Lv$, where v is the velocity of neutrons in the neutron guide, and l is the total length of the neutron guide ($l > L$).

2. EXPERIMENT

The VCN channel which we have employed is shown in Fig. 5. As in our previous work,[1,2] the channel was in the form of bright-dipped copper tubes, whose diameter was up to 200 mm. The channel length was about 13.5 m. The low mean reactor power enabled us to mount different converters cooled with liquid nitrogen including a polyethylene converter which operated for the full reactor cycle (about one month) without substantial radiation damage. The VCN detector was an $LiOH \cdot H_2O + ZnS(Ag)$ scintillation counter having an area of about 25 cm^2.[1] The background was measured by covering the detector with a 10-μ thick copper foil. With the polyethylene converter at $T_C = 300°K$, the VCN counting rate for a reactor power of 25 kW ($\Phi_0 = 3.6 \times 10^{10}$ neutron/$cm^2 \cdot$sec) was 0.30 ± 0.01 sec^{-1}. The elementary theory of diffusion with diffusion parameters as reported in[2] ($L \approx 10$ m, $D \approx 3.4$ $m^2 \cdot sec^{-1}$) gives a reduction in the VCN flux due to the neutron guide by a factor of about 3. Measurements show that the efficiency of our $LiOH \cdot H_2O + ZnS(Ag)$ detector is 0.2—0.25.[11] Bearing this in mind, the expected VCN counting rate agrees with the measured values to within the accuracy of our estimates (~ 50%).

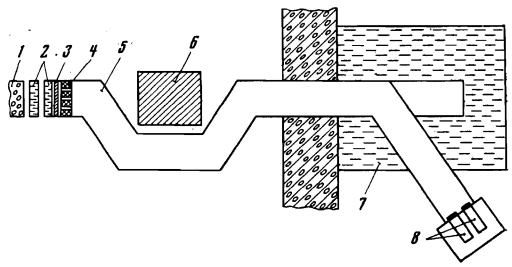

FIG. 5. VCN channel scheme for the IBR-30 pulsed reactor. 1—active zone of the reactor, 2—water moderator, 3—converter, 4—additional moderator, 5—copper neutron guide, 6, 7—shield and direct beam trap, 8—VCN deflectors.

TABLE VI. VCN yield for some converters relative to polyethylene at $T_c = T_n = 300°K$

Converter	Eq. (10)	Experiment
$ZrH_{1.6}$*	0.9	1.0±0.1
Mg	0.414	0.48±0.07
Al	0.087	0.096±0.014

*Experiment data obtained with $ZrH_{1.9}$.

In our geometry (Fig. 5), the thermal-neutron flux at the converter can be substantially increased by mounting an additional moderator inside the neutron guide. The extraction of the VCN from the converter is then achieved through special apertures in this additional moderator, which are lined with bright-dipped copper foil. The VCN output was measured with an additional polyethylene moderator, 100 mm thick, mounted inside the channel and containing 23 apertures, 20 mm in diameter. According to[3], the thermal-neutron flux in this case was increased by a factor of 7 (in the region of the converter) as compared with the case when there was no additional moderator. The use of this moderator resulted in an increase in the VCN yield by a factor of approximmately 2.5 when the total areas of the apertures was ~ 23% of the cross-sectional area of the channel.

Table VI shows the VCN yield of some of the converters relative to the VCN yield of polyethylene, which has practically no potential barrier (as in the case of zirconium hydride, it is assumed that U_c is zero for polyethylene). We note that when the VCN yield was calculated from Eq. (2), $\alpha \approx 0.3$ was used, which was deduced from our data[2] on the mean VCN velocity in the neutron guide.

The cooling of the polyethylene converter from room temperature (300°K) to 130 and 90°K led to an increase in the VCN flux by factors of 2.2 ± 0.2 and 4 ± 0.2, respectively, which is somewhat less than the calculated values (respectively by factors of 3 and 5.5). A similar effect was observed in the cooling of zirconium hydride: a reduction in the converter temperature from room temperature to 130°K led to an increase in the VCN flux by a factor of 2.3 ± 0.2, which is also lower than the calculated value (about 3.4). The possible reason for the discrepancy between experiment and theory is the elastic scattering of VCN by the converter nuclei. However, our estimates have shown that, even in the case of hydrogen at 0°K, the VCN elastic scattering effect can modify the VCN yield by only 10%.

A more substantial effect on the VCN during the reduction in temperature may be due to the presence of inhomogeneities, with sizes of the order the VCN wavelength, in the converter. The VCN yield should decrease as a result of elastic scattering by such inhomogeneities. The increase in the total interaction cross section for slow neutrons, and the sharp deviation of σ_t from the 1/v law (by factors of 2—3), was detected previously for a number of materials.[12]

Of course, the discrepancy with the experimental data may be partly due to the approximate nature of the calculations, for example, due to uncertainties in the frequency spectrum for polyethylene and zirconium hydride, especially since we used the frequency spectra obtained at $T_c \approx 300°K$. The absence of data on frequency spectra for these media at low temperatures prevented us from estimating their effect on the VCN yield.

We note in conclusion that it was shown experimentally in our previous work[2] that the cooling of the aluminum converter down to liquid nitrogen temperatures did not affect the VCN flux to within 30%.

[1] V. I. Lushchikov, Yu. N. Pokotilovskiĭ, A. V. Strelkov, and F. L. Shapiro, ZhETF Pis. Red. 9, 40 (1969) [JETP Lett. 9, 23 (1969)].
[2] L. V. Groshev, V. N. Dvoretskiĭ, A. M. Demidov, Yu. N. Panin, V. I. Lushchikov, Yu. N. Pokotilovskiĭ, A. V. Strelkov, and F. L. Shapiro, JINR Preprint R3-5392, Dubna, 1970.
[3] V. V. Golikov, Zh. A. Kozlov, L. K. Kul'kin, L. B. Pikel'ner, V. T. Rudenko, and É. I. Sharapov, Soobshcheniya OIYaI 3-5736 (JINR Communications 3-5736) Dubna, 1971.
[4] R. Golub, Phys. Lett. 38A, 177 (1972).
[5] V. F. Turchin, Medlennye neĭtrony (Slow Neutrons), Gosatomizdat, 1963.
[6] H. R. Donner, G. J. Safford, H. Boutin, and M. Berger, J. Chem. Phys. 40, 1417 (1964). B. Wunderlich, J. Chem. Phys. 37, 1207 (1962).
[7] J. Young and J. Koppel, Phys. Rev. 134, A1476 (1964).
[8] R. Stedman, L. Almqvist, and G. Nilsson, Phys. Rev. 162, 549 (1967).
[9] V. G. Liforov, M. N. Nikolaev, V. Z. Nozik, V. A. Parfenov, V. A. Semenov, and V. F. Turchin, Inelastic Scattering of Neutrons in Solids and Liquids, Vienna, Vol. 2, 1965, p. 317.
[10] D. J. Hughes and R. Schwartz, Neutron Cross Sections, Brookhaven Nat'l. Laboratory, 1958.
[11] A. V. Strelkov, Abstract of Author's Dissertation 3-5937, Dubna, 1971.
[12] A. Steyerl, Transmissionsmessungen mit ultrakalten Neutronen, Diss. TU Münich, February, 1971.

Translated by S. Chomet
6